

Asymmetry of the neutrino mean free path in hot neutron matter under strong magnetic fieldsJulio Torres Patiño,¹ Eduardo Bauer,^{1,2,*} and Isaac Vidaña³¹*IFLP, CCT-La Plata, CONICET, Argentina*²*Facultad de Ciencias Astronómicas y Geofísicas, Universidad Nacional de La Plata, Argentina*³*Istituto Nazionale di Fisica Nucleare, Dipartimento di Fisica “Ettore Majorana”, Università di Catania, Via Santa Sofia 64, I-95123 Catania, Italy*

(Received 7 August 2018; revised manuscript received 13 March 2019; published 30 April 2019)

The neutrino mean free path in neutron matter under a strong magnetic field is evaluated for the inelastic scattering reaction and studied as a function of the neutron matter density in the range $0.05 \leq \rho \leq 0.4 \text{ fm}^{-3}$ for several temperatures up to 30 MeV and magnetic field strengths from $B = 0$ up to $B = 10^{18}$ G. Polarized neutron matter is described within the nonrelativistic Brueckner–Hartree-Fock (BHF) approach using the Argonne V18 nucleon-nucleon potential supplemented with the Urbana IX three-nucleon force. The LNS Skyrme interaction is also used to describe polarized neutron matter in the Hartree-Fock approximation. Explicit expressions of the cross section per unit volume for the scattering of a neutrino with a spin up or spin down neutron are derived from the Fermi golden rule. Our results show that the mean free path depends strongly on the angle of the incoming neutrino, leading to an asymmetry in this quantity. This asymmetry depends on the magnetic field intensity and on the density, but it is rather independent of the temperature. For a density of 0.15 fm^{-3} at a temperature $T = 15$ MeV, the asymmetry in the mean free path is found to be, for both models, $\approx 0.2\%$ and $\approx 2\%$ for $B = 10^{16}$ and $B = 10^{17}$ G, respectively, and $\approx 15\%$ ($\approx 26\%$) for the BHF (Skyrme) model for $B = 10^{18}$ G.

DOI: [10.1103/PhysRevC.99.045808](https://doi.org/10.1103/PhysRevC.99.045808)**I. INTRODUCTION**

Neutrinos play a crucial role in the physics of supernova explosions [1–3], during the early evolution of compact stellar remnants [4,5], in neutron star cooling [6,7], and in neutron star mergers [8–10]. A large number of neutrinos are produced by electron capture processes during the gravitational collapse of the core of a massive star. Most of the initial gravitational binding energy is stored and released by the neutrinos. In the early stages following the formation of a neutron star the neutrino mean free path λ decreases and, above a critical value of the density, becomes smaller than the stellar radius. Under these conditions neutrinos are trapped in the star. Neutrino trapping has a strong influence on the overall stiffness of the equation of state (EoS) of dense matter [11,12], being the physical conditions of hot and lepton-rich neutron stars substantially different from those of the cold and deleptonized ones. The cooling of a newly born hot neutron star is driven first by the neutrino emission from the interior. There are several neutrino emission processes that contribute to the cooling of neutron stars. These include among others, the direct and modified URCA processes, bremsstrahlung, and Cooper pair formation, the latter operating only when the temperature of the star drops below the critical temperature for neutron superfluidity or proton superconductivity. A comprehensive and detailed review of neutrino emission processes in neutron stars can be found in Ref. [13]. Neutrino cross sections and emissivity are fundamental inputs for supernova simulations

and cooling calculations. These quantities can be substantially affected by the presence of strong magnetic fields in neutron stars. In the case of the so-called magnetars, the magnetic field intensity can reach values up to 10^{14} – 10^{15} G at the star surface and it can grow by several orders of magnitude in its dense interior [14]. The emission of neutrinos, for instance, is expected to be asymmetric (i.e., to depend on the direction of the neutrino) under the presence of a strong magnetic field.

The asymmetrical emission of neutrinos has been suggested as a possible mechanism to explain the so-called pulsar kick problem: the observation that pulsars do not move with the velocity of its progenitor star, but rather with a substantially greater speed. Although an asymmetry as small as $\approx 1\%$ would be enough to explain the pulsar movement, this mechanism has been questioned as the (unique) source for the pulsar kick (see, for instance, Ref. [15]). Other possible explanatory mechanisms include: an asymmetry in the gravitational collapse of the progenitor, acceleration due to the pulsar electromagnetic radiation, or the evolution of binary system, which may produce rapidly moving pulsars. The asymmetrical emission of neutrinos can have different origins. Neutrino oscillation can be altered by the magnetic field, resulting in an anisotropy in the momentum of the outgoing neutrinos [16]. Parity violation can also induce an asymmetry on the neutrino emission when multiple scattering of neutrinos in slightly polarized neutrons is taken into account [17,18,47]. Here we are particularly interested in this last mechanism, which on practice results from the addition of a modified differential cross section plus the cumulative effect of multiple scattering. In this case, two ingredients are important: the

*Corresponding author: bauer@fisica.unlp.edu.ar

differential cross section and the neutrino mean free path. In the absence of a magnetic field the nonrelativistic elastic differential cross section of neutrinos with neutron matter can be written as,

$$\frac{d\sigma}{d\Omega} = \frac{G_F^2 E_\nu^2}{4\pi^2} [C_A^2(3 - \cos\theta) + C_V^2(1 + \cos\theta)], \quad (1)$$

where G_F is the Fermi coupling constant and θ is the scattering angle. Even though the differential cross section is not uniform, in the absence of a preference spatial axis, the average emission of neutrinos from the whole neutron star would be isotropic. However, the presence of a magnetic field modifies this expression and produces an asymmetry in the neutrino emission.

The second ingredient, the neutrino mean free path in dense matter (defined as the inverse of the total neutrino cross section per unit volume) has been studied in the absence of a magnetic field by many authors using various approximation schemes and various models of the trapping environment (see, e.g., Refs [19–32] and references therein). The behavior of neutrinos in dense matter under the presence of strong magnetic fields has been also considered in the literature [15–17,33–40]. However, the asymmetry on the neutrino emission, due to the breaking of the isotropy by the field, has not been discussed much.

The scope of the present work is to analyze the effect of a strong magnetic field on the mean free path of neutrinos in hot neutron matter focusing, in particular, on the asymmetry on the neutrino emission induced by the presence of the field. In neutron matter the two dominant mechanisms contributing to the neutrino mean free path are the scattering of the neutrino with a neutron and the absorption of the neutrino by the neutron producing a proton and an electron in the final state. In this work, however, we will restrict ourselves to the first one of these mechanisms. The interested reader is referred, e.g., to Ref. [24] for a complete description of all possible reactions involving neutrinos.

In particular, we derive explicit expressions of the neutrino cross section per unit volume for the scattering of a neutrino with a spin up or spin down neutron. The description of polarized neutron matter is made within the nonrelativistic Brueckner–Hartree-Fock (BHF) approach using the Argonne V18 [41] nucleon-nucleon potential supplemented with the Urbana IX [42] three-nucleon force. The LNS Skyrme interaction [43] is also used to describe polarized neutron matter in the Hartree-Fock approximation.

The paper is organized as follows. In Sec. II, we discuss the inelastic scattering neutrino cross section with polarized neutrons. Starting from the Fermi golden rule, we develop expressions for the total neutrino cross section, taking the nonrelativistic limit to be consistent with our models for the polarized neutron matter EoS. Our results are presented in Sec. III where we start discussing the properties of polarized neutron matter, some generalities of the neutrino mean free path, and we finish showing the asymmetry of this quantity induced by the presence of a magnetic field. Finally, in Sec. IV a summary, the main conclusions and future perspectives are given.

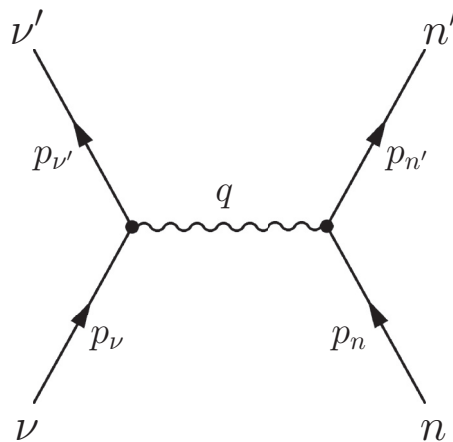


FIG. 1. The lowest-order Feynman diagram for the scattering reaction $\nu + n \rightarrow \nu' + n'$. The quantities p_i and q denote, respectively, the four-momentum of the involved particles and the corresponding four-momentum transfer by the interaction.

II. NEUTRINO CROSS SECTION

In this section we derive the expression for the neutrino total cross section per unit volume in hot neutron matter under the presence of a strong constant magnetic field. As it has already been said in Sec. I, in this work we restrict ourselves to the neutrino scattering process,

$$\nu + n \rightarrow \nu' + n', \quad (2)$$

denoting ν and n (ν' and n') the incoming (outgoing) neutrino and neutron, respectively. We note here that in this work neutrinos are considered massless. Figure 1 shows the lowest-order Feynman diagram contributing to this reaction. Using the Fermi golden rule (see, e.g., Ref. [44]), we can write down the contribution of this reaction to the total cross section per unit volume simply as:

$$\begin{aligned} \frac{\sigma(p_\nu)}{V} &= \int \frac{d\vec{p}_{\nu'}}{(2\pi)^3} \int \frac{d\vec{p}_n}{(2\pi)^3} \int \frac{d\vec{p}_{n'}}{(2\pi)^3} \\ &\times (2\pi)^4 \delta^{(4)}(p_\nu + p_n - p_{\nu'} - p_{n'}) \\ &\times f_n(\vec{p}_n, T) (1 - f_{n'}(\vec{p}_{n'}, T)) \frac{\langle |\mathcal{M}_{\nu'n',\nu n}|^2 \rangle}{2^4 E_\nu E_{\nu'} E_n E_{n'}}, \end{aligned} \quad (3)$$

where $p_i = (E_i, \vec{p}_i)$ is the four-momentum of particle i , $\mathcal{M}_{\nu'n',\nu n}$ is the so-called Møller invariant transition matrix, which we discuss below, the symbol $\langle \rangle$ denotes a sum over final spins and an average over initial ones, and $f_i(\vec{p}_i, T)$ is the particle distribution function, which in thermal equilibrium is given by the Fermi–Dirac one,

$$f_i(\vec{p}_i, T) = \frac{1}{1 + \exp[(E_i(\vec{p}_i, T) - \mu_i(T))/T]}, \quad (4)$$

being E_i the single-particle energy of neutron i , μ_i its chemical potential, and T the temperature of the system. The single-particle energy E_i and the chemical potential μ_i should be obtained from a particular model of neutron matter. In what follows and for convenience, we discuss first the total neutrino

cross section for a system of unpolarized neutrons and then we consider the polarized case.

A. Neutrino cross section for an unpolarized system

The two ingredients necessary to obtain the neutrino total cross section for an unpolarized system of neutrons are the invariant transition matrix $\mathcal{M}_{\nu n', \nu n}$, and a model for the EoS of neutron matter. The first of them describes a two-body process mediated by the weak interaction, whereas the second one characterizes the state of the strongly interacting neutron system, and is obtained by solving the complicated many-body problem. We focus now on the evaluation of the matrix $\mathcal{M}_{\nu n', \nu n}$. Here we show the main steps on the derivation and we refer the interested reader to the Appendix A for specific details. Our starting point is the following Lagrangian density written in terms of a current-current interaction as:

$$\mathcal{L} = \frac{1}{\sqrt{2}} G_F (\bar{\psi}_{\nu'} \gamma^\mu (1 - \gamma_5) \psi_\nu) (\bar{\psi}_{n'} \gamma_\mu (C_V - C_A \gamma_5) \psi_n). \quad (5)$$

Here $G_F \simeq 1.436 \times 10^{-49}$ erg cm⁻³ is the Fermi weak coupling constant and the quantities $C_V = -1/2$ and $C_A = -1.23/2$ are the vector and axial-vector couplings, respectively. The matrix $\mathcal{M}_{\nu n', \nu n}$ can be written from this Lagrangian density as:

$$\mathcal{M}_{\nu n', \nu n} = \frac{1}{\sqrt{2}} G_F (\bar{u}_{\nu'} \gamma^\mu (1 - \gamma_5) u_\nu) (\bar{u}_{n'} \gamma_\mu (C_V - C_A \gamma_5) u_n). \quad (6)$$

It is convenient to express the square of this matrix as the contraction of a leptonic ($l^{\mu\alpha}$) and an hadronic ($H_{\mu\alpha}$) two-rank tensor,

$$|\mathcal{M}_{\nu n', \nu n}|^2 = \frac{1}{2} G_F^2 l^{\mu\alpha} H_{\mu\alpha}, \quad (7)$$

with

$$l^{\mu\alpha} = (\bar{u}_{\nu'} \gamma^\mu (1 - \gamma_5) u_\nu) (\bar{u}_{\nu'} \gamma^\alpha (1 - \gamma_5) u_\nu), \quad (8)$$

and

$$H_{\mu\alpha} = (\bar{u}_n (C_V + C_A \gamma_5) \gamma_\mu u_{n'}) (\bar{u}_{n'} \gamma_\alpha (C_V - C_A \gamma_5) u_n). \quad (9)$$

If neutron matter is not polarized then $\langle |\mathcal{M}_{\nu n', \nu n}|^2 \rangle$ (and consequently $\sigma(p_\nu)/V$) can be simply obtained from Eqs. (8) and (9). However, the presence of a magnetic field induces a (partial) spin polarization of the system. Since our final aim is to consider the total neutrino cross section over polarized neutrons, it is convenient to write the hadronic tensor $H_{\mu\alpha}$ as sum of two terms by employing the spin projection operator, $\Lambda_s = \frac{1}{2}(1 + \gamma_5 \psi_s)$, with the four-vector $w_s = (0, 0, 0, s)$, which projects into the spin up ($s = +1$) or spin down ($s = -1$) configuration. Using the identity operator, written as $\mathcal{I} = \Lambda_{+1} + \Lambda_{-1}$, in Eq. (9), we have,

$$H_{\mu\alpha} = H_{\mu\alpha}^+ + H_{\mu\alpha}^-, \quad (10)$$

where,

$$H_{\mu\alpha}^s = (\bar{u}_n \Lambda_s (C_V + C_A \gamma_5) \gamma_\mu u_{n'}) (\bar{u}_{n'} \gamma_\alpha (C_V - C_A \gamma_5) \Lambda_s u_n). \quad (11)$$

The hadron tensor is defined for the spin wave functions of the particles involved in the scattering process. If the neutron initial spin state is polarized with spin up (down), then the total hadron tensor is reduced to $H_{\mu\alpha}^+$ ($H_{\mu\alpha}^-$). In other words, Eq. (10) does not represent a spin summation of two states (one with spin up and the other with spin down), but the up and down projection of one wave function into its spin up and down components. The spin summation over final states and the average over the initial ones is performed afterwards. From this, it is convenient to work separately with $H_{\mu\alpha}^+$ and $H_{\mu\alpha}^-$. By contracting these hadronic tensors with the leptonic one, we obtain the matrices $|\mathcal{M}_{\nu n', \nu n}^+|^2$ and $|\mathcal{M}_{\nu n', \nu n}^-|^2$. The derivation is developed in Appendix A, where we present explicit expressions for both $\langle |\mathcal{M}_{\nu n', \nu n}^\pm|^2 \rangle$. Furthermore, in this Appendix, we show some prescriptions to obtain their nonrelativistic limit, whose final results are,

$$\begin{aligned} \langle |\mathcal{M}_{\nu n', \nu n}^+|^2 \rangle &= 16 G_F^2 m_N^2 E_\nu E_{\nu'} ((C_V^2 + 3C_A^2) + (C_V^2 - C_A^2) \cos \theta_{\nu\nu'}) \\ &\quad + 2C_A ((C_A + C_V) \cos \theta_\nu + (C_V - C_A) \cos \theta_{\nu'}) \end{aligned} \quad (12)$$

and

$$\begin{aligned} \langle |\mathcal{M}_{\nu n', \nu n}^-|^2 \rangle &= 16 G_F^2 m_N^2 E_\nu E_{\nu'} ((C_V^2 + 3C_A^2) + (C_V^2 - C_A^2) \cos \theta_{\nu\nu'}) \\ &\quad - 2C_A ((C_A + C_V) \cos \theta_\nu + (C_V - C_A) \cos \theta_{\nu'}). \end{aligned} \quad (13)$$

By construction, these expressions do not depend on the momentum of the incoming and outgoing neutron. Similar expressions can be found in other works (see, e.g., Refs. [35,37]). Note that in Eqs. (12) and (13), we have already performed the summation on final spins. As shown in Eq. (2), in the initial state we have a neutrino and a neutron. We are considering massless neutrinos, which are left handed (or polarized). Analogously, in Eqs. (12) and (13), we have also a defined state of polarization for the neutron. In an unpolarized system we assume that it is equally likely to have the neutron with spin up, as to have it with spin down. Therefore, the average between these two states is simply, $\langle |\mathcal{M}_{\nu n', \nu n}|^2 \rangle = (\langle |\mathcal{M}_{\nu n', \nu n}^+|^2 \rangle + \langle |\mathcal{M}_{\nu n', \nu n}^-|^2 \rangle)/2$. We have then,

$$\begin{aligned} \langle |\mathcal{M}_{\nu n', \nu n}|^2 \rangle &= 16 G_F^2 m_N^2 E_\nu E_{\nu'} ((C_V^2 + 3C_A^2) \\ &\quad + (C_V^2 - C_A^2) \cos \theta_{\nu\nu'}). \end{aligned} \quad (14)$$

The average leads to the cancellation among the terms proportional to $\cos \theta_\nu$ and $\cos \theta_{\nu'}$, which are present in Eqs. (12) and (13).

By replacing Eq. (14) into Eq. (3), we have,

$$\begin{aligned} \frac{\sigma(p_\nu)}{V} &= G_F^2 \int \frac{d\vec{p}_{\nu'}}{(2\pi)^3} (C_V^2 (1 + \cos \theta_{\nu\nu'}) \\ &\quad + C_A^2 (3 - \cos \theta_{\nu\nu'})) \mathcal{S}^0(q_0, \vec{q}, T), \end{aligned} \quad (15)$$

where we have used the function $\delta^{(3)}(\vec{p}_\nu + \vec{p}_n - \vec{p}_{\nu'} - \vec{p}_{n'})$ to integrate over the momentum $\vec{p}_{n'}$ of the outgoing neutron. $\mathcal{S}^0(q_0, \vec{q}, T)$ is the structure function describing the response of neutron matter to the excitations induced by neutrinos,

which reads:

$$\mathcal{S}^0(q_0, \vec{q}, T) = \frac{1}{(2\pi)^2} \int d\vec{p}_n f_n(\vec{p}_n, T) (1 - f_n(\vec{p}_n + \vec{q}, T)) \times \delta[q_0 + E_n(\vec{p}_n, T) - E_n(\vec{p}_n + \vec{q}, T)], \quad (16)$$

being $q_0 = E_v - E_{v'}$ and $\vec{q} = \vec{p}_v - \vec{p}_{v'}$. The cross section in Eq. (15), is the expression frequently found in the literature. Note that the neutrino mean free path is simply $\lambda = (\sigma/V)^{-1}$. To evaluate Eq. (15) we use single-particle energies and chemical potentials from an EoS model. Details on this point are given in the next section.

B. Neutrino cross section for a polarized system

Note that not only the $\mathcal{M}_{\nu\nu', \nu n}^\pm$ matrices are different for neutrons with spin up and down, but that the single-particle energies required for the evaluation of the structure function have also a spin dependence for spin polarized systems. Let us start, therefore, our discussion of the neutrino cross section for a polarized system by analyzing first some general features of the EoS.

In this work, to describe the bulk and single-particle properties of neutron matter under the presence of a strong magnetic field we use the BHF approximation of the Brueckner-Bethe-Goldstone (BBG) nonrelativistic many-body theory of nuclear matter and also the Hartree-Fock one with a Skyrme interaction. A detailed description of both EoS approaches can be found in Ref. [45] and references therein. It is worth to mention that the inputs for these two EoS models are the neutron density, the temperature, and the magnitude of the magnetic field. By a minimizing process, both EoS models give as a result the values for the single-particle energies of neutrons with spin up and down, their chemical potentials (which have no spin dependence, as we show below) and the spin asymmetry A that describes the degree of polarization of the system, defined as

$$A = \frac{\rho_+ - \rho_-}{\rho_+ + \rho_-}, \quad (17)$$

with ρ_+ (ρ_-) being the density of neutrons with spin up (down). The value $A = 0$ corresponds to unpolarized neutron matter, whereas $A = +1$ or $A = -1$ means that the system is in a completely polarized state with all the spins up or down, respectively. Partially polarized states correspond to values of A between -1 and $+1$. The degree of spin polarization corresponding to the actual physical state of the system is obtained by minimizing the following thermodynamic potential per unit volume,

$$\mathcal{U} = \mathcal{F} - \vec{\mathcal{M}} \cdot \vec{B}, \quad (18)$$

with respect to A for fixed values of the density, the temperature and the magnetic field. In the above expression \mathcal{F} and $\vec{\mathcal{M}}$ are, respectively, the Helmholtz free energy density and the magnetization per unit volume of the system. This minimization implies that in the physical state the chemical potential of neutrons with spin up and spin down is the same, i.e., there is only one chemical potential that is associated to the conservation of the total baryonic number. In the following lines we explicitly demonstrate this last statement.

The chemical potentials of neutrons with spin up and down is simply given by

$$\mu_s = \frac{\partial \mathcal{U}}{\partial \rho_s}, \quad s = \pm 1. \quad (19)$$

Expressing ρ_+ and ρ_- in terms of the total density $\rho = \rho_+ + \rho_-$ and the spin asymmetry A it is easy to rewrite the chemical potentials as

$$\mu_s = \frac{\partial \mathcal{U}}{\partial \rho} + s \left(\frac{1 - sA}{\rho} \right) \frac{\partial \mathcal{U}}{\partial A}, \quad s = \pm 1. \quad (20)$$

The difference between the two chemical potentials reads simply

$$\mu_+ - \mu_- = \frac{2}{\rho} \frac{\partial \mathcal{U}}{\partial A}, \quad (21)$$

which clearly shows, as we already said that the minimization of \mathcal{U} with respect to A implies the existence of a unique chemical potential in the physical state. Summarizing, given the density, temperature and the magnetic field of the system, from the EoS we obtain the chemical potential, the single-particle energies of the neutrons and the spin asymmetry, which is a global property of the system.

Being, therefore, neutron matter partially polarized under the presence of a magnetic field, we need expressions for the total cross section describing the neutrino scattering with neutrons with either spin up or spin down, $\sigma^\pm(p_\nu)/V$. These expressions are simply obtained by replacing Eqs. (12) and (13), into Eq. (3) reading,

$$\frac{\sigma^\pm(p_\nu)}{V} = G_F^2 \int \frac{d\vec{p}_{v'}}{(2\pi)^3} [(C_V^2 + 3C_A^2) + (C_V^2 - C_A^2) \cos \theta_{vv'}] \pm 2C_A((C_A + C_V) \cos \theta_v + (C_V - C_A) \cos \theta_{v'}) \times \mathcal{S}_\pm^0(q_0, \vec{q}, T), \quad (22)$$

where the kinematical conditions of Eq. (22) are the same as in Eq. (16). Depending on the neutron spin projection, the neutrino mean free path is $\lambda^\pm = (\sigma^\pm/V)^{-1}$. The structure function has now a spin dependence and it is given by,

$$\mathcal{S}_\pm^0(q_0, \vec{q}, T) = \frac{1}{(2\pi)^2} \int d\vec{p}_n f_n^\pm(\vec{p}_n, T) [1 - f_n^\pm(\vec{p}_n + \vec{q}, T)] \times \delta[q_0 + E_n^\pm(\vec{p}_n, T) - E_n^\pm(\vec{p}_n + \vec{q}, T)]. \quad (23)$$

The dependence with the spin projection of the neutron is present in the distribution functions and in the single-particle energies, which, together with the chemical potential, are obtained from the two models of the polarized neutron matter EoS. Within the BHF model, these quantities are employed to evaluate numerically the structure function. At variance, for the Skyrme scheme, an analytical expression of $\mathcal{S}_\pm^0(q_0, \vec{q}, T)$ can be obtained. In this case the single-particle energy for a neutron with spin $s = \pm 1$, in a magnetic field can be written as,

$$E^\pm(\vec{p}, T) = \frac{|\vec{p}|^2}{2m_\pm^*} + U^\pm \mp \kappa B, \quad (24)$$

where m_{\pm}^* is the effective mass of neutrons with spin up or down, U^{\pm} a potential term (see Ref. [45] for an explicit expression), which depends on the density, the temperature, and the magnetic field, but not on the momentum, and $\kappa = -1.913\mu_N$ the anomalous magnetic moment of the neutron in units of the nuclear magneton μ_N . Due to its simplicity, we reproduce here the expression for the effective mass,

$$\frac{1}{m_s^*} = \frac{1}{m_N} + \frac{1}{4} \rho (b_0 + s b_1 A). \quad (25)$$

As before, we have $s = 1(-1)$ for spin up (down). The constants $b_0 = t_1(1 - x_1) + 3t_2(1 + x_2)$ and $b_1 = t_2(1 + x_2) - t_1(1 - x_1)$, are written in terms of the standard parameters of the Skyrme model, t_1 , t_2 , x_1 , and x_2 .

The quadratic dependence of the neutron single-particle energies leads, in the case of Skyrme model, to the following analytic expression for the structure function (see, e.g., Refs. [28,30,32]):

$$S_{\pm}^0(q_0, \vec{q}, T) = \frac{1}{\pi} \frac{1}{1 - e^{-q_0/T}} \frac{(m_{\pm}^*)^2 T}{4\pi q} \ln \left(\frac{1 + e^{(A_{\pm} + q_0/2)/T}}{1 + e^{(A_{\pm} - q_0/2)/T}} \right), \quad (26)$$

where $A_{\pm} = \mu_{\pm} - m_{\pm}^* q_0^2/2q^2 - q^2/8m_{\pm}^*$ and $\mu_{\pm} \equiv \mu - U^{\pm} \pm \kappa B$ with μ being the neutron chemical potential, which in the physical state, as shown before, is independent of the spin orientation.

Before we discuss our numerical results for the neutrino mean free path λ , it is worth to make some general considerations on Eq. (22). Let us consider first the nonpolarized limit ($A = 0$). Averaging on spin from Eq. (22) and having in mind that without polarization we have $S_{-}^0 = S_{+}^0 = S^0$, it is easy to obtain the nonpolarized cross section [Eq. (15)].

From a comparison of Eq. (15) with Eq. (22), we see that they differ in the terms proportional to $\cos \theta_v$ and $\cos \theta_{v'}$. These terms are due to the neutron polarization. Since the integration is done over $\vec{p}_{v'}$, the contribution to the cross section from the term proportional to $\cos \theta_{v'}$ is almost negligible. Even though it is not zero, since S_{\pm}^0 itself depends implicitly on $\cos \theta_{v'}$ through the transfer momentum \vec{q} , which involves the angle $\theta_{vv'}$, whose cosine can be easily written as (see Fig. 2),

$$\cos \theta_{vv'} = \sin \theta_v \sin \theta_{v'} \cos \phi_{v'} + \cos \theta_v \cos \theta_{v'}. \quad (27)$$

It is obvious that the cross section depends on the energy and momentum of the incoming neutrino. Note, in particular that if the momentum of the incoming neutrino is perpendicular to the magnetic field then $\cos \theta_v = 0$ and one expects no appreciable differences with respect to the unpolarized case.

As a final comment for this section, we should call attention to our initial hypothesis about the uniform character of the magnetic field. We have made this assumption to evaluate the cross section of a neutrino with a single neutron. The use of a dipole magnetic field for the whole neutron star could be a possible choice for the geometry of the field. The curvature of such a field would allow us to consider it as locally uniform due to the scale of the neutrino–neutron scattering process. However, the potential use of our results in a realistic code for the diffusion of neutrinos in a neutron star, should care about the curvature of the field by assigning a particular direction

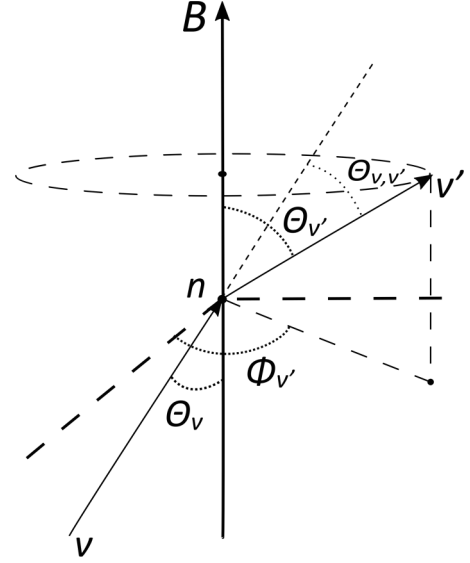


FIG. 2. Geometry of the scattering process. The magnetic field defines the z axis. The incoming neutrino, ν , has polar angle θ_ν and without loss of generality we take its azimuthal angle ϕ_ν equal to zero. For the outgoing neutrino ν' , we have a polar angle $\theta_{\nu'}$ and an azimuthal angle $\phi_{\nu'}$. The angle between ν and ν' is $\theta_{\nu\nu'}$ defined through Eq. (27). Note that we have neglected the neutron momenta.

and strength to the magnetic field, according to the position where the scattering takes place. Similar considerations can be made for the density and the temperature, as this region should be small compared to the whole neutron star, but big enough to get a local solution of the EoS.

III. RESULTS AND DISCUSSION

In the following we present results for the mean free path of neutrinos in homogeneous hot neutron matter under the presence of strong magnetic fields. Results are shown for densities in the range $0.05 \leq \rho \leq 0.4 \text{ fm}^{-3}$ corresponding approximately to the outer core region a neutron star, several temperatures up to $T = 30 \text{ MeV}$, and different values of the magnetic field intensity ranging from $B = 0$ up to $B = 10^{18} \text{ G}$. As we have already mentioned, our description of the bulk and single-particle properties of hot and magnetized neutron matter is mainly based on the nonrelativistic BHF approach developed in Ref. [45] using, in particular, the Argonne V18 nucleon-nucleon potential [41] supplemented with the Urbana IX three-nucleon force [42]. In addition, in order to set a comparison with another model, we show also some results for the LNS Skyrme interaction developed by Cao *et al.* [43]. We have employed this particular parametrization of the Skyrme interaction as it is specially suitable for a comparison with the BHF model since its parameters were determined by fitting the nuclear matter EoS calculated in the BHF framework.

Before discussing our results for the neutrino mean free path, we analyze first the spin asymmetry A of the system, and the structure function $S_{\pm}^0(q_0, \vec{q}, T)$ for different temperatures and magnetic field intensities. As it was mentioned in the previous section, the spin asymmetry A characterizes the

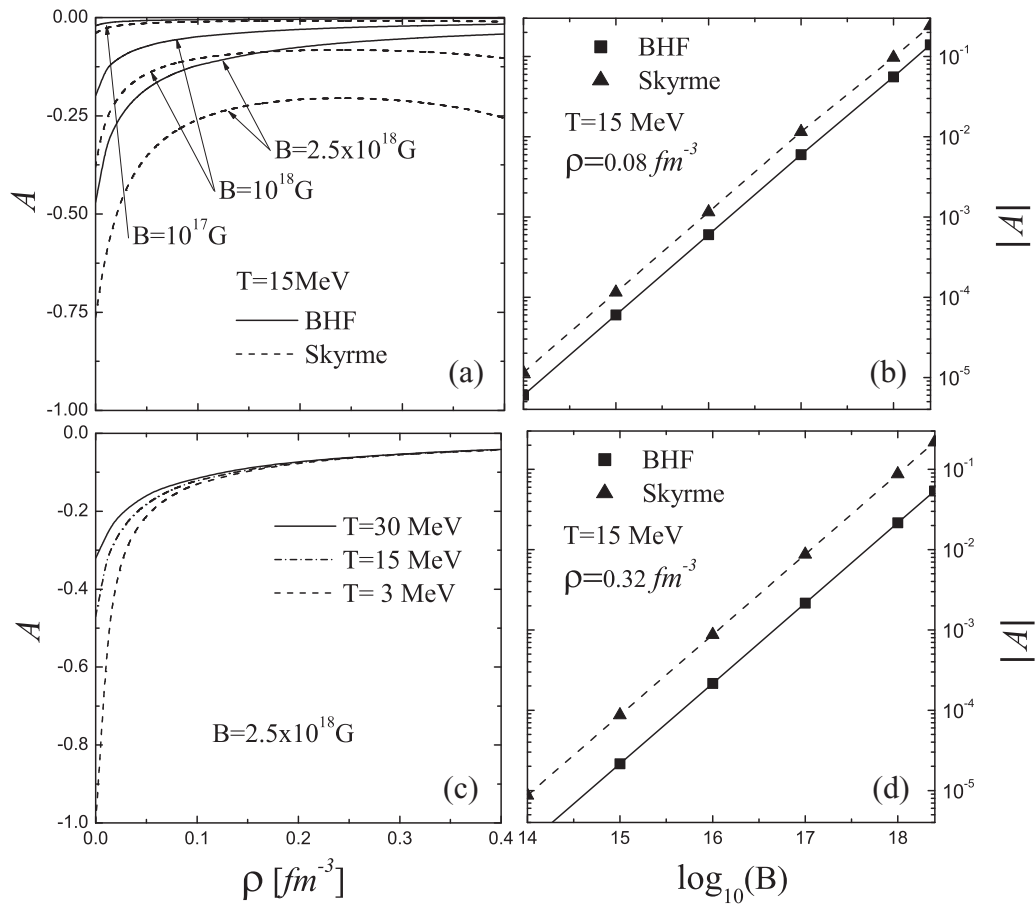


FIG. 3. Dependence of the spin asymmetry A on density and magnetic field strength. Its density dependence is shown in (a) and (c), for different values of the magnetic field strength and different values of the temperature, respectively. The spin asymmetry behavior with the magnitude of the magnetic field is depicted in (b) and (d), for two different values of the density.

degree of polarization of the system. We note that the degree of polarization of the physical state of the system is the result of the competition between the strong interaction that, together with the temperature, favor the nonpolarized state as the physical one, and the magnetic field that tries to align all the neutron spins antiparallel to it. In Figs. 3(a) and 3(c) we show the spin asymmetry corresponding to the physical state of the system as a function of density for several temperatures and magnetic field intensities for both models, BHF (solid lines) and Skyrme (dashed lines), of the polarized neutron matter EoS. Although it is not shown in the figure, in the absence of a magnetic field the physical state of the system corresponds to the nonpolarized case ($A = 0$) for all densities and temperatures. For low densities and temperatures, one expects that the system would be completely polarized ($A = -1$) up to a given density, above which it becomes partially polarized with a predominance of spin down states ($-1 < A < 0$). The system is always more polarized in the case of Skyrme. Within our range of temperatures, A grows monotonously and the system would reach the nonpolarized state ($A = 0$) asymptotically at high densities for the BHF model. This is not the case for most of the Skyrme interactions, which exhibit a so-called ferromagnetic instability at high densities ($A = -1$). There is a general consensus nowadays that the prediction of this instability is in fact a pathology of Skyrme

forces. In Fig. 3(a), one notices a decrease of A (i.e., becomes more negative) at high densities, which would lead to this instability. Up to the densities that we have analyzed, the overall impact on our final results is small and a particular study of the different Skyrme interactions goes beyond the scope of the present contribution. As mentioned, our main concern is the results within the BHF model, which does not show this problem.

On the other hand, a comparison of the results for $B = 10^{17}$ G, 10^{18} G, and 2.5×10^{18} G [see Fig. 3(a)]¹ shows a significant decrease in the spin asymmetry at low densities as the magnetic field grows. Eventually, at a very low density it can turn into a system with complete polarization ($A = -1$). Referring now to the temperature dependence and as it is seen in Fig. 3(c), the increase of temperature makes the system to be less polarized as one intuitively expects since it favors the disorder of the spins. The dependence of the spin asymmetry with the magnetic field strength is shown in Figs. 3(b) and 3(d). Since the spin asymmetry A is negative,

¹In this figure and in the next two, we have included a magnetic field intensity of $B = 2.5 \times 10^{18}$ G, a value that is rather high. This has been done only to show, in a clearer way, the effect of the magnetic field.

for simplicity we have plotted the absolute value of A in a logarithmic scale as a function of the logarithm of the strength of the field. Results are shown for both models of the EoS for $T = 15$ MeV and two densities $\rho = 0.08$ fm $^{-3}$ [Fig. 3(b)] and $\rho = 0.32$ fm $^{-3}$ [Fig. 3(d)]. The spin asymmetry increases (in absolute value) with the strength of the field, being always larger for the Skyrme interaction. These figures suggest that in the logarithmic scale, $|A|$ exhibits a linear dependence with $\log_{10} B$. Moreover, within the range of the variables considered, the slope of the lines seem to be the same for both models, being approximately equal to one. We can not give a simple explanation for this behavior, but we should stress that the spin asymmetry saturates at $|A| = 1$. Therefore, for the lowest densities or for arbitrarily high magnetic fields, this linear behavior is lost. We should point out that for all models one has $A = 0$ for $B = 0$, a point that can not be drawn in a logarithmic scale. In addition, these two panels show that the spin asymmetry becomes significant only for magnetic fields larger than $\approx 10^{17}$ G as it can be seen also in Fig. 3(a).

Let us now give some insight into the effect of the structure function $S_{\pm}^0(q_0, \vec{q}, T)$, defined in Eq. (23), on the neutrino mean free path. In Fig. 4 we show $S_{\pm}^0(q_0, \vec{q}, T)$ as a function of q_0 for a density of the system $\rho = 0.16$ fm $^{-3}$. The momentum transfer is fixed to the value $\vec{q} = \vec{p}_v/2$ where the magnitude of the momentum of the incoming neutrino \vec{p}_v has been taken according to the prescription $|\vec{p}_v| = 3T$. Results in the absence of a magnetic field for temperatures $T = 3$ and $T = 15$ MeV are shown in Fig. 4(a) whereas in Fig. 4(b) the structure function is shown for $T = 15$ MeV and magnetic fields $B = 0$ G (which will serve as a reference) and $B = 2.5 \times 10^{18}$ G. As it is seen in Fig. 4(a), an increase of the temperature leads to a much broader structure function with a larger area under it. The reason is simply due to the fact that the phase space of the integral in Eq. (23) increases with temperature. Consequently, an increase of the temperature will give rise to a larger cross section and, therefore, to a smaller neutrino mean free path when integrating Eq. (22), as we will see later. Besides the dependence of the structure function on q_0 , \vec{q} , and T , from its definition [see Eq. (23)], it is clear that it depends also on the spin projection of the neutrons. This, as it is observed in Fig. 4(b), leads to a splitting between $S_{+}^0(q_0, \vec{q}, T)$ and $S_{-}^0(q_0, \vec{q}, T)$, with $S_{+}^0(q_0, \vec{q}, T) < S_{-}^0(q_0, \vec{q}, T)$, whose origin is the dependence of the neutron single-particle energy on the spin polarization induced by the presence of the field. The magnetic field polarizes partially the system with a spin asymmetry $-1 < A < 0$ making the single-particle energy for neutrons with spin down (the most abundant component) less attractive than the one for neutrons with spin up. As it is shown in Ref. [46] [see, in particular, Eqs. (23) and (24) of this reference], this is due to: (i) the change in the number of pairs that a neutron with a given momentum and spin projection can form with the other neutrons of the system as neutron matter is polarized, and (ii) to the spin dependence of the in-medium neutron-neutron interaction in the spin polarized system. Indeed, as the spin asymmetry decreases the single-particle energy of a spin down neutron is built from a larger number of down-down pairs that form a spin triplet state $S = 1$ and, due to the Pauli

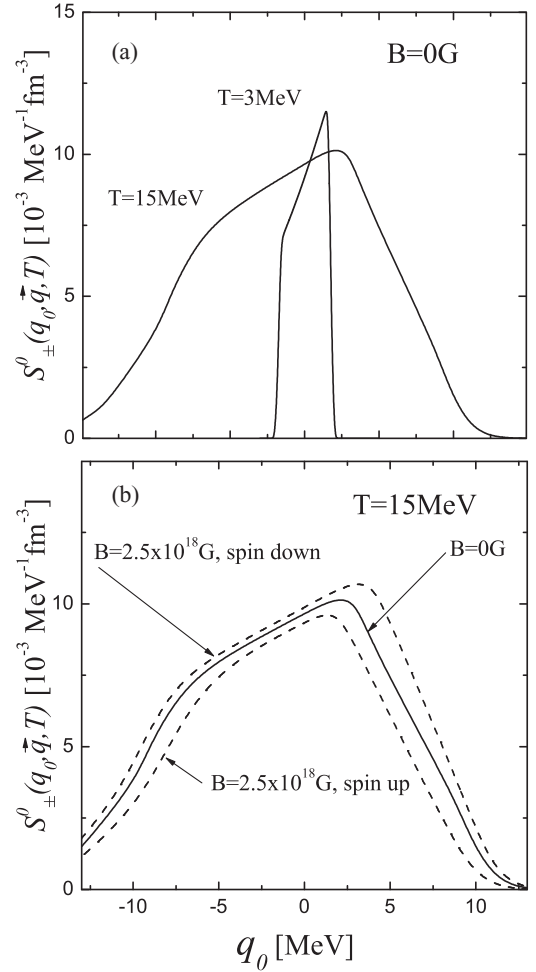


FIG. 4. Energy dependence of the structure function $S_{\pm}^0(q_0, q, T)$ for $\rho = 0.16$ fm $^{-3}$. Results for $B = 0$ G with $T = 3$ MeV and 15 MeV are shown in (a), whereas those for $T = 15$ MeV and $B = 0$ G and $B = 2.5 \times 10^{18}$ G are presented in (b). In both panels the momentum transfer is fixed to the value $\vec{q} = \vec{p}_v/2$ with $|\vec{p}_v| = 3T$.

principle, can only interact through odd angular momentum partial waves. Conversely, the potential of the less abundant component is built from a relatively larger number of up-down pairs that can interact both in the $S = 0$ and $S = 1$ channels. Thus, the potential of the less abundant component receives also contributions from some important attractive channels as, e.g., the 1S_0 . In the end, all this makes the phase space of neutrons with spin up to be smaller than that of neutrons with spin down and, therefore, after integrating Eq. (23) one finds $S_{+}^0(q_0, \vec{q}, T) < S_{-}^0(q_0, \vec{q}, T)$. Therefore, an increase of the magnetic field strength will lead to a decrease (increase) of the scattering cross section σ_{+} (σ_{-}) of the neutrino with a spin up (down) neutron and, consequently, to an increase (decrease) of λ_{+} (λ_{-}). This is illustrated in Fig. 5, where we show λ_{\pm} as a function of density for $T = 3$ MeV, two values of the magnetic field $B = 0$ G and $B = 2.5 \times 10^{18}$ G, and an angle of the incoming neutrino $\theta_v = \pi/2$. Note that in the absence of magnetic field we have, $\lambda_{+} = \lambda_{-}$, represented by the continuous line in the figure. Note also that the difference

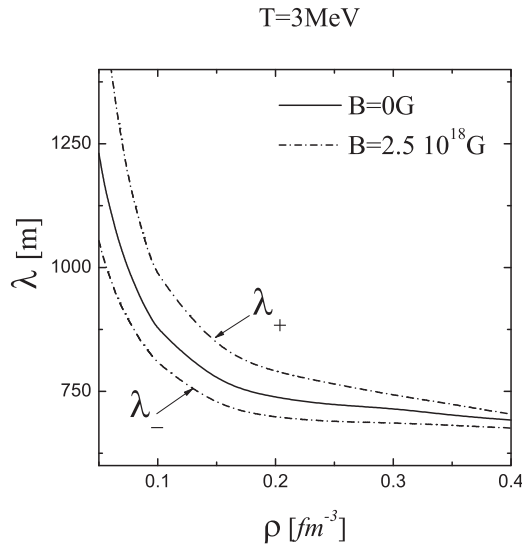


FIG. 5. Neutrino mean free path as a function of the density at $T = 3$ MeV for $B = 0$ G and $B = 2.5 \times 10^{18}$ G within the BHF-model. The angle between the incoming neutrino and the magnetic field is taken at $\theta_v = \pi/2$. For the momentum of the incoming neutrino we employ $|\vec{p}_v| = 3T$.

between λ_+ and λ_- is larger for low and medium densities and decreases for the higher ones.

We will focus our discussion now on the behavior of the neutrino mean free path. Before starting our analysis, however, we would like to make a general remark. Note that in the absence of a magnetic field the total cross section [see Eq. (15)] depends only on the magnitude of the momentum of the incoming neutrino, but not on its direction. The reason is simply that one can always take the \hat{z} axis along the direction of the outgoing neutrino to perform the integral and, therefore, the angle $\theta_{v'}$ between the direction of both neutrinos is integrated out. This is not the case when the magnetic field is different from zero. Its presence establishes a preferred direction in space and consequently, the total cross section [see Eq. (22)] depends both on the magnitude of the momentum of the incoming neutrino and on the angle θ_v between its momentum \vec{p}_v and the direction of the magnetic field. It is interesting to note, however, that if \vec{p}_v is perpendicular to the magnetic field (i.e., $\theta_v = \pi/2$) then the neutrino mean free path is expected to have a weak dependence with the magnetic field. The reason is that when $\theta_v = \pi/2$, the term proportional to $\cos \theta_{v'}$ in Eq. (22) would cancel out except for the smooth implicit $\theta_{v'}$ dependence of the structure function through the angle $\theta_{v'}$ [see Eq. (27)], which, however, is negligible for $\theta_v = \pi/2$. The only dependence on the magnetic field that remains is, therefore, that of the structure function itself, which is mostly appreciable in the low-medium density region where the spin asymmetry A is smaller [i.e., more negative, see Figs. 3(a) and 3(c)]. This is shown in Fig. 5, for the extreme case of $B = 2.5 \times 10^{18}$ G. More details on this point are given soon, when we discuss the results for $\theta_v \neq \pi/2$.

We analyze now the temperature dependence of the neutrino mean free path and to simplify the discussion, we will consider only the BHF-model, since the results using the

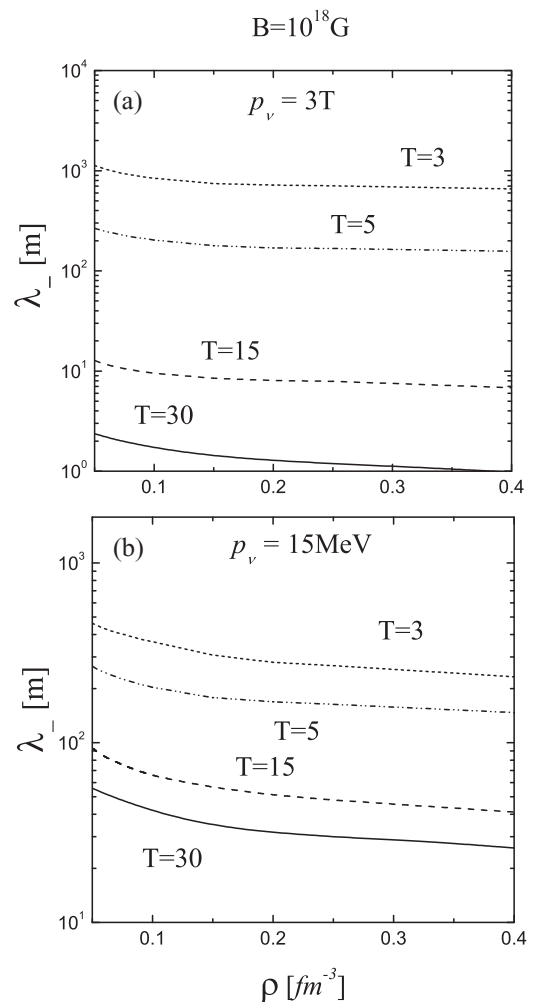


FIG. 6. Neutrino mean free path as a function of the density at $B = 10^{18}$ G and $\theta_v = \pi/2$ for several values of the temperature within the BHF-model. We consider neutrons with spin down. For the momentum of the incoming neutrino we take $|\vec{p}_v| = 3T$ in (a) and $|\vec{p}_v| = 15$ MeV in (b). All results are evaluated using the BHF-model.

Skyrme-model are similar. In addition, we show only to the λ_- , as the behavior of λ_+ is qualitatively the same and its analysis would add nothing different. In Fig. 6, we show the density dependence of λ_- for a magnetic field strength $B = 10^{18}$ G, $\theta_v = \pi/2$, and the temperatures $T = 3, 5, 15$, and 30 MeV. The momentum of the incoming neutrino is taken $|\vec{p}_v| = 3T$ in Fig. 6(a) and $|\vec{p}_v| = 15$ MeV in Fig. 6(b). As it is seen in both panels, λ_- varies dramatically with temperature, decreasing up to four orders of magnitude [see Fig. 6(a)] for increasing values of the temperature. This can be easily understood from our previous analysis of the temperature dependence of the structure function $S_{\pm}^0(q_0, \vec{q}, T)$. As we just saw, a larger temperature implies a larger phase space of the integral in Eq. (23), and, therefore, a larger (smaller) total cross section (neutrino mean free path). Taking into account that the typical radius of a neutron star is of the order of 10–12 km, from these results one can easily conclude that a neutrino would unlikely interact with matter at low

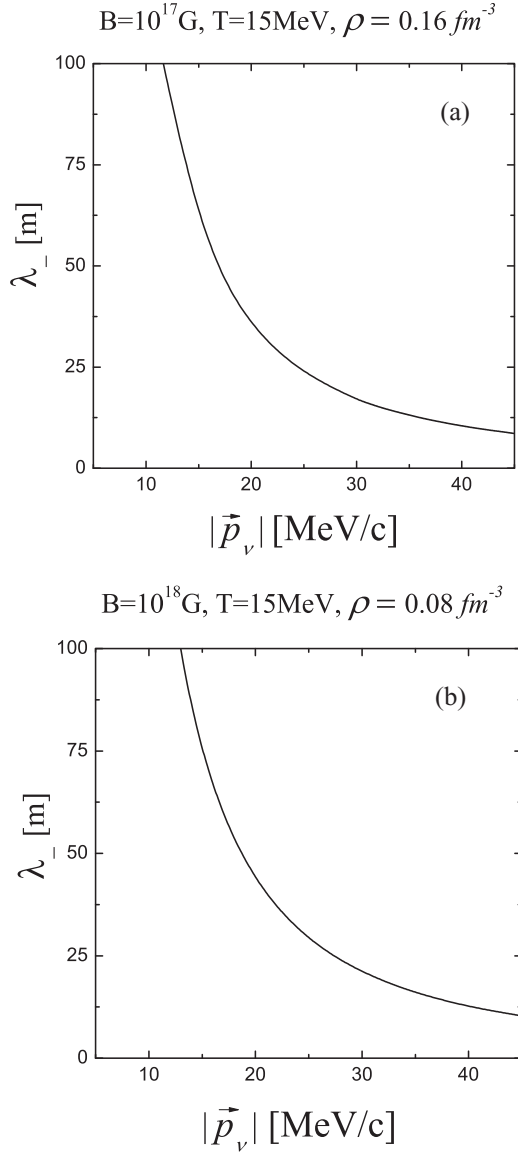


FIG. 7. Neutrino mean free path as a function of the momentum of the incoming neutrino, $|\vec{p}_\nu|$ for $\theta_\nu = \pi/2$, within the BHF-model. We consider neutrons with spin down. In (a) we present results for $B = 10^{17}$ G and for $B = 10^{18}$ G in (b). In addition, we have chosen three values for the angle of the incoming neutrino. Note that the $|\vec{p}_\nu|$ scale is different among the two panels.

temperatures. From this, we can say that from temperatures starting around $T = 10$ MeV, one has to care of the neutrino scattering. Moreover, for $T = 30$ MeV, multiple scattering should be considered.

Also Fig. 6 indicates that at a fixed temperature, for larger values of $|\vec{p}_\nu|$, one obtains smaller results for the neutrino mean free path. In Fig. 7 we explore this behavior by fixing the temperature at $T = 15$ MeV and considering $B = 10^{17}$ G and $\rho = 0.16 \text{ fm}^{-3}$ in Fig. 7(a), while in Fig. 7(b) these values are set at $B = 10^{18}$ G and $\rho = 0.08 \text{ fm}^{-3}$. We limit ourselves again to λ_- with $\theta_\nu = \pi/2$ and with the BHF model as a representative case. We observe that the mean free path decrease for increasing values of $|\vec{p}_\nu|$. This is due to the fact that the

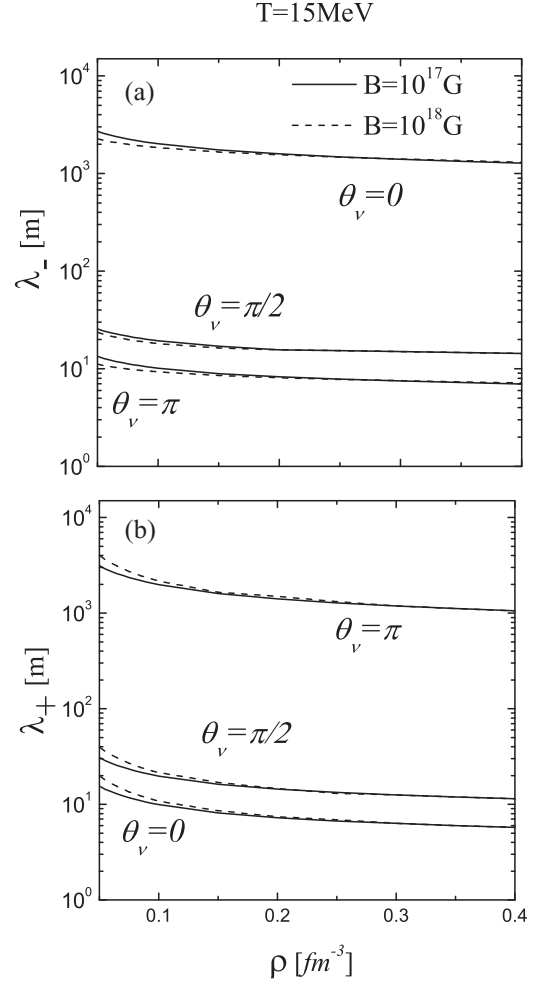


FIG. 8. Neutron spin down (λ_-) and spin up (λ_+) partial contribution to the mean free path within the BHF model. We set the temperature at $T = 15$ MeV, while the magnetic field is $B = 10^{17}$ G and $B = 10^{18}$ G. Three different values for θ_ν are considered. The momentum of the incoming neutrino is $|\vec{p}_\nu| = 3T$.

response of the system to the excitations induced by neutrinos, described by the structure function, is larger for larger values of the neutrino momentum. Consequently, the total cross section is larger and the neutrino mean free path smaller.

As a next point, we examine the dependence of the neutrino mean free path on the angle θ_ν . The contributions λ_- and λ_+ to the neutrino mean free path are respectively shown in Figs. 8(a) and 8(b), as a function of the density for $T = 15$ MeV, $B = 10^{17}$ G, and 10^{18} G and the angles $\theta_\nu = 0, \pi/2$ and π , within the BHF model. We note first that both contributions vary by more than two orders of magnitude with the angle θ_ν . This huge variation cannot be understood by considering only the explicit angular factors in Eq. (22), but it results from the combined effect of these factors and the implicit angular dependence of the structure function. In polarized neutron matter, neutrons with spin down (up) are almost transparent to the neutrinos if the incoming angle of the latter is $\theta_\nu = 0$ (π). Note also that λ_- (λ_+) is shorter for $\theta_\nu = \pi$ (0).

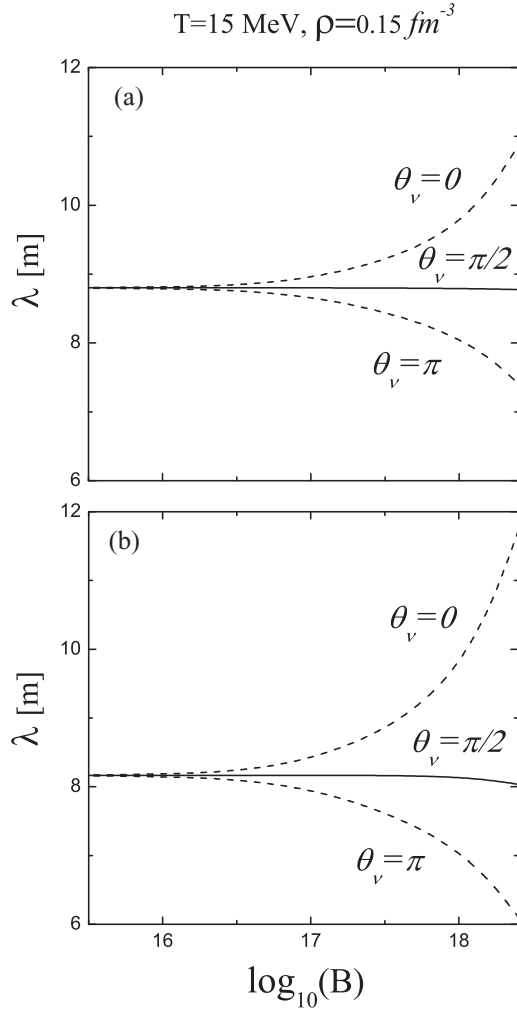


FIG. 9. Total neutrino mean free path dependence with the magnetic field strength for three angles of the incoming neutrino. Results for the BHF and Skyrme models are shown in (a) and (b), respectively.

Up to now, we have analyzed the contributions to the neutrino mean free path due to the scattering of the neutrino with spin up or spin down neutrons. However, under the presence of a magnetic field neutron matter is partially polarized. In Appendix B, we have developed a model for the total cross section, which takes care of the partial polarization of the system. The total neutrino mean free path is obtained from Eq. (B10), having,

$$\lambda(p_\nu) = \frac{2\lambda_+(p_\nu)\lambda_-(p_\nu)}{(1-A)\lambda_+(p_\nu) + (1+A)\lambda_-(p_\nu)}. \quad (28)$$

In what follows, the reader should have in mind this expression when we refer to the total neutrino mean free path.

In Fig. 9, we show in two panels the total neutrino mean free path as a function of the magnetic field strength. This is done for $T = 15$ MeV and a density $\rho = 0.15 \text{ fm}^{-3}$. We also assume the condition $|\vec{p}_\nu| = 3T$. We present results for both BHF and Skyrme models, in Figs. 9(a) and 9(b), respectively. We observe, as it was mentioned before, a negligible B -

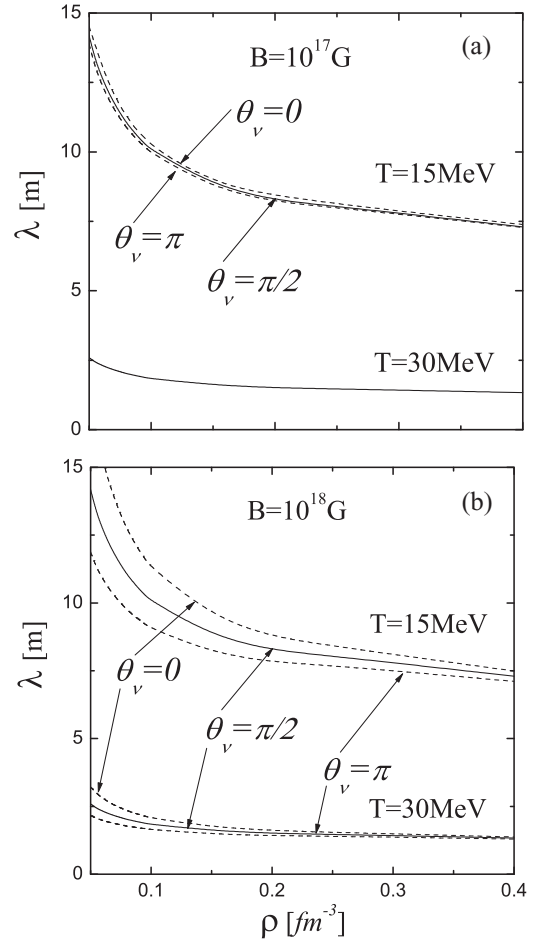


FIG. 10. Dependence of the total neutrino mean free path within the BHF model. We show the dependence with the angle between the incoming neutrino and the magnetic field, θ_ν , for two values of the temperature and two values of the magnetic field intensity. The momentum of the incoming neutrino is $|\vec{p}_\nu| = 3T$.

dependence of the neutrino mean free path for $\theta_\nu = \pi/2$. The situation is different for all other angles: we depict results only for the extreme cases $\theta_\nu = 0$ and $\theta_\nu = \pi$. We observe an increase of the mean free path for $\theta_\nu = 0$, as the magnetic field grows. This means that it becomes more unlikely that the neutrino interacts with a neutron. The opposite situation occurs for $\theta_\nu = \pi$. The results for both models are similar, but as expected within the Skyrme model the change in the mean free path for increasing values of B , is more pronounced than with the BHF model. Also from this figure and in a somehow arbitrary way, one can assert that the splitting in the neutrino mean free path for different θ_ν values, becomes relevant from $B \approx 10^{17}$ G.

Finally, we show in Figs. 10 and 11 the total mean free path for two magnetic field intensities, two temperatures, and three angles for the BHF-model and the Skyrme scheme, respectively. It is clear from our previous analysis that the asymmetry in the mean free path comes from the spin asymmetry factor A and the spin dependence of the structure functions \mathcal{S}_\pm^0 . Neutrinos are more transparent to polarized neutron matter when moving in a direction parallel to the magnetic

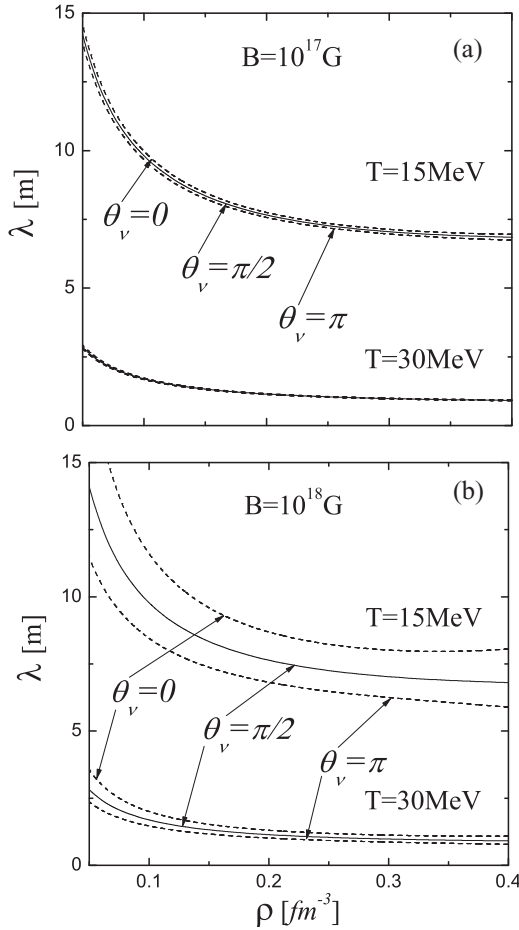


FIG. 11. The same as Fig. 10, but for the Skyrme model.

field ($\theta_v = 0$). The situation is the opposite for neutrinos that move in an antiparallel direction ($\theta_v = \pi$). In order to get a better understanding on this asymmetry in the mean free path, we define a mean free path asymmetry, as follows:

$$\chi_\lambda = \frac{\lambda(\theta_v = 0) - \lambda(\theta_v = \pi)}{\lambda(\theta_v = \pi/2)}. \quad (29)$$

In practice, $\lambda(\theta_v = \pi/2)$ can be considered as the average value between the two extreme ones. In Table I, we show some representative values for this ratio. Even though the asymmetry is rather small, specially for $B = 10^{16}$ G, a small asymmetry in the emission of neutrinos would have a significant physical impact in a compact object. The asymmetry

TABLE I. Mean free path asymmetry χ_λ , as a function of the density at $T = 15$ MeV, for three values of the magnetic field intensity. These results are rather independent of the temperature.

ρ [fm $^{-3}$]	$\chi_\lambda(B = 10^{16}G)$		$\chi_\lambda(B = 10^{17}G)$		$\chi_\lambda(B = 10^{18}G)$	
	BHF	Skyrme	BHF	Skyrme	BHF	Skyrme
0.050	0.0032	0.0036	0.0322	0.0357	0.2705	0.3647
0.150	0.0021	0.0023	0.0232	0.0257	0.1516	0.2657
0.400	0.0019	0.0027	0.0151	0.0311	0.0519	0.3212

is specially relevant for low to medium densities. This is so because of the dependence of the spin asymmetry parameter A on the density (see Fig. 3). As the density increases, the action of the nuclear strong interaction among the neutrons overcomes the coupling of the neutrons with the magnetic field. Although this is a general behavior for all EoS models, we should mention that the use of the Skyrme model leads to a bigger asymmetry for the mean free path, as it is shown in the table. This is obviously due to the larger spin asymmetry predicted by the Skyrme model.

At this point, we would like to mention that in a potential stellar evolution code, one possible scheme would be to consider that the neutrinos interact with neutrons either with spin up or spin down. Therefore, the partial contributions to the total mean free path shown in Fig. 8, should be employed in the calculation. We refer to a semiphenomenological model where one keeps track of an individual neutrino, using mean free path and differential cross sections evaluated with quantum mechanics. As already mentioned, in this case one should care about the direction of the magnetic field in each particular location. Another model would be to employ Eq. (28), using local values of the density, temperature, and magnetic field, all quantities that vary according to the position in the neutron star. In fact, the EoS is obtained assuming infinite neutron matter and one should model the star by assigning local values for the single-particle energies, chemical potential, and spin asymmetry, according to the local point under consideration.

In reference to others works on the subject, we should mention the contribution by Maruyama *et al.* [47], where the neutrino cross section through the direct URCA process is calculated in proto-neutron-star matter in the presence of a magnetic field $B = 10^{17}$ G. This calculation is performed within an EoS obtained with a relativistic mean field approach. The magnetic field is also locally uniform, by assuming a uniform dipole magnetic field along the z direction, i.e., $\mathbf{B} = B\hat{z}$. In that work, results for the neutrino production and the absorption during transport are given. The overall effect is that the magnetic field increases the momentum flux of neutrinos parallel to the magnetic field, while it does the opposite for neutrinos moving antiparallel to the field. Due to the different physical processes involved, a quantitative comparison with our contribution is not feasible, but we have arrived at the same qualitative result.

As a final comment for this section, we would like to call attention to the different interactions involved in the evaluation of the neutrino mean free path. First, the scattering matrix is governed by the weak interaction. We make now some considerations on the strong interaction. In this contribution we have discussed results from the BHF and the Skyrme models: mainly, the differences between these results come from the different strong interactions employed. At this point it is worth to mention the work by Rrapaj *et al.* [48], where it is calculated the neutrino absorption rates due to charged-current reactions using a realistic nucleon-nucleon interaction that fit measured scattering phase shifts. This interaction is employed to evaluate the nucleon self-energy within the Hartree-Fock approximation in a self-consistent way starting from a realistic nucleon-nucleon interaction without a strong repulsive core derived in the framework of chiral effective field theory at the

N^3 LO in the chiral expansion. This approach is conceptually quite similar to the BHF one employed in the present work, the main difference being the use of the more traditional Argonne V18 two-body and Urbana IX three-body forces to build up the G matrices, which describe the in-medium nucleon-nucleon interaction and have a regular behavior even for strong short-range repulsions. Unfortunately, the physical process and conditions are different than ours, which does not allow a comparison among both results. Also referring to the strong interaction, its effect beyond the mean field can be also important: the so-called ring approximation (see for instance Refs. [39,40]) is perhaps the simplest way to account for the effect of the strong interaction beyond the mean field. In this case an effective nuclear interaction is employed, leading in general to some reduction in the structure function. From this, one can conclude that the choice for the strong interaction and how the strong interaction is implemented within the calculation is an important issue. Even though our results for both models show some consistency, we consider that this point deserves further attention.

IV. SUMMARY, CONCLUSIONS, AND FUTURE PERSPECTIVES

In this work we have evaluated the neutrino mean free path in neutron matter under the presence of a strong magnetic field. The description of polarized neutron matter has been done within the nonrelativistic Brueckner–Hartree-Fock (BHF) approach using the Argonne V18 nucleon-nucleon potential supplemented with the Urbana IX three-nucleon force, and within a Hartree-Fock approximation using the LNS Skyrme interaction. We have considered only the neutrino scattering process. Starting from the Fermi golden rule we have derived explicit expressions of the neutrino cross section per unit volume for the scattering of a neutrino with a spin up or spin down neutron. These expressions have been obtained in the nonrelativistic limit to be consistent with our description of polarized neutron matter. We have shown that in the presence of a magnetic field the neutrino mean free path depends on the angle between the momentum of the incoming neutrino \vec{p}_ν , and the magnetic field, leading to an asymmetry in this quantity.

In previous works by other authors, the asymmetry in the neutrino emission refers to the one originated from the differential cross section. This asymmetry and the one we have considered here are different and should be considered simultaneously to account for the actual asymmetric neutrino emission. In principle, all differential cross sections are asymmetric. However, in the absence of a preference spacial axis, the average emission from the compact object is isotropic. We have shown that this situation is altered by the presence of a magnetic field. One should be aware that the mean free path is the relevant variable in this problem: for low temperatures, the mean free path can be much larger than the size of the compact object itself. In this case, the asymmetry in the differential cross section would not be relevant, as it would be unlikely to have a collision. The total cross section (which is the inverse of the mean free path), erases the angular information of the differential cross section. That is, the asymmetry in

the mean free path has a different origin than the one from the differential cross section. While the last one gives us information on the way in which the weak interaction scatters the neutrinos, the mean free path tells us about how often a neutrino interacts with a neutron.

In this analysis the temperature is the key variable. In the early stages of the cooling process of a neutron star, the temperature is high enough to ensure several collisions of the neutrinos with the neutrons before the neutrino leaves the star. It would be interesting to analyze how the asymmetry in the mean free path affects the cooling processes. This analysis is, however, beyond the scope of the present work since among other things one should also consider the absorption cross section, where the neutrino is absorbed by the neutron, having a proton and an electron as the final state. The inclusion of this process is not straightforward as protons and electrons show Landau levels in a magnetic field. We are presently working to include this mechanism.

As a final comment, we believe that the asymmetric emission of neutrinos from a magnetar has still several unexplored issues, which can be relevant for the problem of the pulsar kick. In this work we have explored just one of them, namely, the asymmetry in the mean free path. Apart from the absorption cross section just mentioned, another interesting point is the effect of the strong interaction over the structure function. To the best of our knowledge, this has been done only up to the ring-approximation level, as discussed in the last section. Our aim for the near future is to include the absorption cross section in conjunction with the asymmetry in the differential cross section to get a better understanding of the asymmetric emission of neutrinos from a magnetar.

ACKNOWLEDGMENTS

This work was partially supported by the CONICET, Argentina, under contract PIP00273, and by “PHAROS: The multimessenger physics and astrophysics of neutron stars”, COST Action CA16214.

APPENDIX A: EVALUATION OF $\langle |\mathcal{M}_{\nu n',vn}|^2 \rangle$

In this Appendix we show some details on the evaluation of the $\mathcal{M}_{\nu n',vn}$ -matrix. We recall its expression from Eq. (6),

$$\mathcal{M}_{\nu n',vn} = \frac{1}{\sqrt{2}} G_F (\bar{u}_{\nu'} \gamma^\mu (1 - \gamma_5) u_\nu) (\bar{u}_{n'} \gamma_\mu (C_V - C_A \gamma_5) u_n). \quad (\text{A1})$$

In the calculation of the neutrino cross section, we need to evaluate,

$$|\mathcal{M}_{\nu n',vn}|^2 = \frac{1}{2} G_F^2 l^{\mu\alpha} H_{\mu\alpha}, \quad (\text{A2})$$

where $l^{\mu\alpha}$ and $H_{\mu\alpha}$ are the leptonic and hadronic tensors, respectively. To perform the spin summation we employ the so-called Casimir’s trick (see for instance Ref. [49]), which allows us to do the spin summations by the evaluation of a trace of matrices. We introduce two traces $L^{\mu\alpha}$ and $\mathcal{H}_{\mu\alpha}$ from the leptonic and hadronic tensors, respectively. Explicit expressions are given soon. We have,

$$\langle |\mathcal{M}_{\nu n',vn}|^2 \rangle = \frac{1}{2} G_F^2 L^{\mu\alpha} \mathcal{H}_{\mu\alpha}. \quad (\text{A3})$$

Let us recall that we sum over the final spin states, but we average over the initial ones. Details on the average over the initial spin states are given in the main text. Now we analyze each trace separately.

1. Leptonic trace

The leptonic tensor is

$$l^{\mu\alpha} = [\bar{u}_{\nu'} \gamma^\mu (1 - \gamma_5) u_\nu]^\dagger [\bar{u}_{\nu'} \gamma^\alpha (1 - \gamma_5) u_\nu]. \quad (\text{A4})$$

Using standard properties of the γ matrices, the adjoint factor of this tensor can be expressed as,

$$[\bar{u}_{\nu'} \gamma^\mu (1 - \gamma_5) u_\nu]^\dagger = u_\nu^\dagger [\gamma^\mu (1 - \gamma_5)]^\dagger \bar{u}_{\nu'}^\dagger = \bar{u}_\nu \gamma^\mu (1 - \gamma_5) u_{\nu'}, \quad (\text{A5})$$

in this way, we have,

$$l^{\mu\alpha} = \bar{u}_\nu \gamma^\mu (1 - \gamma_5) u_{\nu'} \bar{u}_{\nu'} \gamma^\alpha (1 - \gamma_5) u_\nu. \quad (\text{A6})$$

From the so-called Casimir's trick, we can write,

$$\sum_{\text{spins}} l^{\mu\alpha} = L^{\mu\alpha} \quad (\text{A7})$$

where,

$$\begin{aligned} L^{\mu\alpha} &= \text{tr}[\gamma^\mu (1 - \gamma_5) \not{p}_{\nu'} \gamma^\alpha (1 - \gamma_5) \not{p}_\nu] \\ &= 2 \text{tr}(\gamma^\mu \not{p}_{\nu'} \gamma^\alpha \not{p}_\nu + \gamma_5 \gamma^\mu \not{p}_{\nu'} \gamma^\alpha \not{p}_\nu). \end{aligned} \quad (\text{A8})$$

In this expression we have neglected the neutrino mass. After some algebra, we obtain,

$$L^{\mu\alpha} = 8(p_{\nu'}^\mu p_\nu^\alpha + p_\nu^\mu p_{\nu'}^\alpha - g^{\mu\alpha} (p_\nu \cdot p_{\nu'}) - i\epsilon^{\mu\alpha\gamma\lambda} p_{\nu'}^\gamma p_{\nu\lambda}). \quad (\text{A9})$$

2. Hadronic trace

We follow similar steps as in the case of the leptonic trace, but the evaluation is more complex as we have to distinguish two terms, according to the spin projection of the neutron. The hadronic tensor is,

$$H_{\mu\alpha}^s = [\bar{u}_{n'} \gamma_\mu (C_V - C_A \gamma_5) \Lambda_s u_n]^\dagger [\bar{u}_{n'} \gamma_\alpha (C_V - C_A \gamma_5) \Lambda_s u_n], \quad (\text{A10})$$

where, as stated in the main text, we have introduced the spin projection operator over the initial neutron as, $\Lambda_s = (1 + \gamma_5 \not{w}_s)/2$, where $w_s = (0, 0, 0, s)$ with $s = +1$ (-1) for spin up (down). We rewrite the adjoint factor of the hadronic tensor as,

$$[\bar{u}_{n'} \gamma_\mu (C_V - C_A \gamma_5) \Lambda_s u_n]^\dagger = \bar{u}_n \gamma^0 \Lambda_s^\dagger [\gamma_\mu (C_V - C_A \gamma_5)]^\dagger \gamma^0 u_{n'}, \quad (\text{A11})$$

by making the substitution,

$$\gamma^0 \Lambda_s^\dagger [\gamma_\mu (C_V - C_A \gamma_5)]^\dagger \gamma^0 = \Lambda_s (C_V + C_A \gamma_5) \gamma_\mu, \quad (\text{A12})$$

we have,

$$H_{\mu\alpha}^s = \bar{u}_n \Lambda_s (C_V + C_A \gamma_5) \gamma_\mu u_{n'} \bar{u}_{n'} \gamma_\alpha (C_V - C_A \gamma_5) \Lambda_s u_n. \quad (\text{A13})$$

As in the leptonic case, the spin summation of this expression leads to the hadronic trace,

$$\begin{aligned} \mathcal{H}_{\mu\alpha}^s &= \text{tr}(\Lambda_s (C_V + C_A \gamma_5) \gamma_\mu (\not{p}_{n'} + m_N) \gamma_\alpha \\ &\quad \times [C_V - C_A \gamma_5] \Lambda_s (\not{p}_n + m_N)). \end{aligned} \quad (\text{A14})$$

To evaluate this trace, we choose the rest frame where the incident neutron is at rest. In this frame we have $[\Lambda_s, \not{p}_n] = 0$. By using the standard rules for traces, together with the property of the projection operator, $(\Lambda_s)^2 = \Lambda_s$, the hadronic trace can be rewritten as,

$$\begin{aligned} H_{\mu\alpha}^s &= \text{tr}[(C_V + C_A \gamma_5) \gamma_\mu (\not{p}_{n'} + m_N) \gamma_\alpha (C_V - C_A \gamma_5) \\ &\quad \times \frac{(1 + \gamma_5 \not{w}_s)}{2} (\not{p}_n + m_N)]. \end{aligned} \quad (\text{A15})$$

For convenience, we split this trace into three contributions proportional to C_V^2 , C_A^2 , and $C_V C_A$, respectively. Developing each of these contributions we have,

$$\begin{aligned} \mathcal{H}_{\mu\alpha}^{s,V} &= 2C_V^2 ((p_{n'}^\mu p_{n\alpha} + p_{n'}^\alpha p_{n\mu} - g_{\mu\alpha} (p_{n'} \cdot p_n) + m_N^2 g_{\mu\alpha}) \\ &\quad + im_N (\epsilon_{\mu\alpha\gamma\lambda} w^\gamma p_n^\lambda - \epsilon_{\mu\alpha\gamma\lambda} p_{n'}^\lambda w^\gamma)), \\ \mathcal{H}_{\mu\alpha}^{s,A} &= 2C_A^2 ((p_{n'}^\mu p_{n\alpha} + p_{n'}^\alpha p_{n\mu} - g_{\mu\alpha} (p_{n'} \cdot p_n) - g_{\mu\alpha} m_N^2) \\ &\quad - im_N (\epsilon_{\mu\alpha\gamma\lambda} w^\lambda p_{n'}^\gamma + \epsilon_{\mu\alpha\gamma\lambda} p_{n'}^\gamma w^\lambda)), \\ \mathcal{H}_{\mu\alpha}^{s,VA} &= 4C_V C_A (-m_N (p_{n'}^\mu w_\alpha + p_{n'}^\alpha w_\mu - g_{\mu\alpha} (p_{n'} \cdot w)) \\ &\quad - i\epsilon_{\mu\alpha\gamma\lambda} p_{n'}^\gamma p_n^\lambda), \end{aligned} \quad (\text{A16})$$

where for simplicity we have omitted the spin index in all w . So we have,

$$\mathcal{H}_{\mu\alpha}^s = \mathcal{H}_{\mu\alpha}^{s,V} + \mathcal{H}_{\mu\alpha}^{s,A} + \mathcal{H}_{\mu\alpha}^{s,VA}. \quad (\text{A17})$$

It is convenient to give explicit expressions for each spin component. To this end, we employ the explicit values for $w_s = (0, 0, 0, s)$. We also employ the following properties, $\epsilon_{\mu\alpha\gamma\lambda} w^\lambda = s\epsilon_{\mu\alpha\gamma z}$, and $w_\alpha = g_{\alpha\beta} w^\beta = s g_{\alpha z}$, with $s = +1$ (-1) for spin up (down).

For the spin up terms, we have,

$$\begin{aligned} \mathcal{H}_{\mu\alpha}^{+,V} &= 2C_V^2 ((p_{n'}^\mu p_{n\alpha} + p_{n'}^\alpha p_{n\mu} - g_{\mu\alpha} (p_{n'} \cdot p_n) + m_N^2 g_{\mu\alpha}) \\ &\quad + im_N (\epsilon_{\mu\alpha 3\lambda} p_n^\lambda - \epsilon_{\mu\alpha 3\gamma} p_{n'}^\gamma)), \\ \mathcal{H}_{\mu\alpha}^{+,A} &= 2C_A^2 ((p_{n'}^\mu p_{n\alpha} + p_{n'}^\alpha p_{n\mu} - g_{\mu\alpha} (p_{n'} \cdot p_n) - g_{\mu\alpha} m_N^2) \\ &\quad - im_N (\epsilon_{\mu\alpha 3\lambda} p_{n'}^\lambda + \epsilon_{\mu\alpha 3\lambda} p_n^\lambda)), \\ \mathcal{H}_{\mu\alpha}^{+,VA} &= 4C_V C_A (-m_N (p_{n'}^\mu g_{3\alpha} + p_{n'}^\alpha g_{3\mu} + g_{\mu\alpha} p_{n'}^3) \\ &\quad - i\epsilon_{\mu\alpha\gamma\lambda} p_{n'}^\gamma p_n^\lambda), \end{aligned} \quad (\text{A18})$$

while the spin down terms are,

$$\begin{aligned} \mathcal{H}_{\mu\alpha}^{-,V} &= 2C_V^2 ((p_{n'}^\mu p_{n\alpha} + p_{n'}^\alpha p_{n\mu} - g_{\mu\alpha} (p_{n'} \cdot p_n) + m_N^2 g_{\mu\alpha}) \\ &\quad - im_N (\epsilon_{\mu\alpha 3\lambda} p_n^\lambda - \epsilon_{\mu\alpha 3\gamma} p_{n'}^\gamma)), \\ \mathcal{H}_{\mu\alpha}^{-,A} &= 2C_A^2 ((p_{n'}^\mu p_{n\alpha} + p_{n'}^\alpha p_{n\mu} - g_{\mu\alpha} (p_{n'} \cdot p_n) - g_{\mu\alpha} m_N^2) \\ &\quad + im_N (\epsilon_{\mu\alpha 3\lambda} p_{n'}^\lambda + \epsilon_{\mu\alpha 3\lambda} p_n^\lambda)), \\ \mathcal{H}_{\mu\alpha}^{-,VA} &= 4C_V C_A (m_N (p_{n'}^\mu g_{3\alpha} + p_{n'}^\alpha g_{3\mu} + g_{\mu\alpha} p_{n'}^3) \\ &\quad - i\epsilon_{\mu\alpha\gamma\lambda} p_{n'}^\gamma p_n^\lambda). \end{aligned} \quad (\text{A19})$$

3. Evaluation of $\langle |\mathcal{M}_{\nu n', \nu n}^\pm|^2 \rangle$

Finally, we build up $\langle |\mathcal{M}_{\nu n', \nu n}^\pm|^2 \rangle$. By replacing Eqs. (A9), (A18), and (A19), into Eq. (A3), we have,

$$\begin{aligned} \langle |\mathcal{M}_{\nu n', \nu n}^+|^2 \rangle &= 4G_F^2 (p_{\nu'}^\mu p_\nu^\alpha + p_\nu^\mu p_{\nu'}^\alpha - g^{\mu\alpha} (p_{\nu'} \cdot p_\nu) - i\epsilon^{\mu\alpha\gamma\rho} p_{\nu'\gamma} p_{\nu\rho}) (2(C_V^2 + C_A^2) (p_{n'\mu} p_{n\alpha} + p_{n'\alpha} p_{n\mu} - g_{\mu\alpha} (p_{n'} \cdot p_n)) \\ &\quad + 2(C_V^2 - C_A^2) m_N^2 g_{\mu\alpha} + 2(C_V^2 - C_A^2) i m_N \epsilon_{\mu\alpha 3\theta} p_n^\theta - 2m_N i (C_V^2 + C_A^2) \epsilon_{\mu\alpha 3\lambda} p_{n'}^\lambda \\ &\quad - 4C_V C_A (m_N (p_{n'\mu} g_{3\alpha} + p_{n'\alpha} g_{3\mu} + g_{\alpha\mu} p_{n'}^3) + i\epsilon_{\mu\alpha\lambda\theta} p_{n'}^\lambda p_n^\theta)) \\ \langle |\mathcal{M}_{\nu n', \nu n}^-|^2 \rangle &= 4G_F^2 (p_{\nu'}^\mu p_\nu^\alpha + p_\nu^\mu p_{\nu'}^\alpha - g^{\mu\alpha} (p_{\nu'} \cdot p_\nu) - i\epsilon^{\mu\alpha\gamma\rho} p_{\nu'\gamma} p_{\nu\rho}) (2(C_V^2 + C_A^2) (p_{n'\mu} p_{n\alpha} + p_{n'\alpha} p_{n\mu} - g_{\mu\alpha} (p_{n'} \cdot p_n)) \\ &\quad + 2(C_V^2 - C_A^2) m_N^2 g_{\mu\alpha} - 2(C_V^2 - C_A^2) i m_N \epsilon_{\mu\alpha 3\theta} p_n^\theta + 2m_N i (C_V^2 + C_A^2) \epsilon_{\mu\alpha 3\lambda} p_{n'}^\lambda \\ &\quad + 4C_V C_A (m_N (p_{n'\mu} g_{3\alpha} + p_{n'\alpha} g_{3\mu} + g_{\alpha\mu} p_{n'}^3) - i\epsilon_{\mu\alpha\lambda\theta} p_{n'}^\lambda p_n^\theta)). \end{aligned} \quad (\text{A20})$$

The final step is to perform all contractions and to take the nonrelativistic limit of these expressions. We do this in two steps. First, we take the neutron at rest (for both the initial and final state). Using this approximation together with the property, $\epsilon^{\xi\phi\gamma\nu} \epsilon_{\lambda\rho\gamma\nu} = -2(\delta_\lambda^\xi \delta_\rho^\phi - \delta_\rho^\xi \delta_\lambda^\phi)$, we obtain,

$$\begin{aligned} \langle |\mathcal{M}_{\nu n', \nu n}^+|^2 \rangle &= 16G_F^2 ((C_V^2 + C_A^2) ((p_{n'} \cdot p_{\nu'}) (p_n \cdot p_\nu) + (p_{n'} \cdot p_\nu) (p_n \cdot p_{\nu'})) - (C_V^2 - C_A^2) m_N^2 (p_\nu \cdot p_{\nu'})) \\ &\quad + C_V^2 m_N (p_{\nu'}^3 (p_\nu \cdot (p_n - p_{n'})) + p_\nu^3 (p_{\nu'} \cdot (p_n - p_n))) + C_A^2 m_N (p_{\nu'}^3 (p_{\nu'} \cdot (p_n + p_{n'})) - p_\nu^3 (p_\nu \cdot (p_n + p_{n'}))) \\ &\quad + 2C_V C_A m_N ((p_{\nu'} \cdot p_{n'}) p_\nu^3 + (p_\nu \cdot p_{n'}) p_{\nu'}^3) \end{aligned} \quad (\text{A21})$$

and

$$\begin{aligned} \langle |\mathcal{M}_{\nu n', \nu n}^-|^2 \rangle &= 16G_F^2 ((C_V^2 + C_A^2) ((p_{n'} \cdot p_{\nu'}) (p_n \cdot p_\nu) + (p_{n'} \cdot p_\nu) (p_n \cdot p_{\nu'})) - (C_V^2 - C_A^2) m_N^2 (p_\nu \cdot p_{\nu'})) \\ &\quad - C_V^2 m_N (p_{\nu'}^3 (p_\nu \cdot (p_n - p_{n'})) + p_\nu^3 (p_{\nu'} \cdot (p_n - p_n))) - C_A^2 m_N (p_{\nu'}^3 (p_{\nu'} \cdot (p_n + p_{n'})) - p_\nu^3 (p_\nu \cdot (p_n + p_{n'}))) \\ &\quad - 2C_V C_A m_N ((p_{\nu'} \cdot p_{n'}) p_\nu^3 + (p_\nu \cdot p_{n'}) p_{\nu'}^3). \end{aligned} \quad (\text{A22})$$

By choosing the z axis along the direction of the magnetic field, the nonrelativistic limit can be obtained by using the following relations:

$$\begin{aligned} (p_n \cdot p_{n'}) &\cong m_N^2 \\ (p_n \cdot p_\nu) &\cong m_N E_\nu \\ (p_n \cdot p_{\nu'}) &\cong m_N E_{\nu'} \\ (p_\nu \cdot p_{n'}) &\cong m_N E_\nu \\ (p_{\nu'} \cdot p_{n'}) &\cong m_N E_{\nu'} \\ (p_\nu \cdot p_{\nu'}) &= E_\nu E_{\nu'} (1 - \cos \theta_{\nu\nu'}) \\ p_\nu^3 &= E_\nu \cos \theta_\nu \\ p_{\nu'}^3 &= E_{\nu'} \cos \theta_{\nu'}, \end{aligned} \quad (\text{A23})$$

where θ_ν ($\theta_{\nu'}$) is the angle between the incoming (outgoing) neutrino with the magnetic field and $\theta_{\nu\nu'}$ is the angle between the direction of the incoming and the outgoing neutrino. The geometry of the scattering process is shown in Fig. 2. The nonrelativistic limits of these equations are given in Eqs. (12) and (13) in the main text.

APPENDIX B: TOTAL NEUTRINO CROSS SECTION FOR A PARTIALLY POLARIZED SYSTEM

In this Appendix we derive an explicit expression for the total neutrino-neutron scattering cross section in partially spin polarized neutron matter. We start by evaluating the spin average of the whole system $\langle \hat{S}_z \rangle_{\text{System}}$, which is simply,

$$\langle \hat{S}_z \rangle_{\text{System}} = \left(\frac{N_+ - N_-}{N_+ + N_-} \right) \frac{\hbar}{2}, \quad (\text{B1})$$

where N_+ and N_- are, respectively, the number of neutrons with spin up and down and \hat{S}_z is the spin projection operator ($\hat{S}_z |\pm\rangle = \pm(\hbar/2) |\pm\rangle$). Writing now $N_\pm = V \rho_\pm$, with V the volume of the system, and using the definition of the spin asymmetry A Given in Eq. (17) is easy to see that,

$$\langle \hat{S}_z \rangle_{\text{System}} = A \frac{\hbar}{2}. \quad (\text{B2})$$

We recall that A is obtained from the minimization of the thermodynamic potential per unit volume defined in Eq. (18).

Let us assume that the system is made of a collection of neutrons, each one of them being in the same mixed state of spin up and spin down. The general mixed spin wave function of each individual neutron is simply,

$$|\chi_n\rangle = \alpha |+\rangle + \beta |-\rangle. \quad (\text{B3})$$

Let $\langle \hat{S}_z \rangle_{\chi_n}$ be the mean spin value of this system of neutrons, we know that this quantity is related with the mean value of a single neutron by, $\langle \hat{S}_z \rangle_{\chi_n} = \langle \chi_n | \hat{S}_z | \chi_n \rangle$ [50]. We have then,

$$\langle \hat{S}_z \rangle_{\chi_n} = (|\alpha|^2 - |\beta|^2) \frac{\hbar}{2}. \quad (\text{B4})$$

As the next step, we make the hypothesis that $\langle \hat{S}_z \rangle_{\chi_n} = \langle \hat{S}_z \rangle_{\text{System}}$. Therefore, we can write,

$$\begin{aligned} |\alpha|^2 - |\beta|^2 &= A \\ |\alpha|^2 + |\beta|^2 &= 1, \end{aligned} \quad (\text{B5})$$

where the second equation simply reflects the normalization condition of the wave function $|\chi_n\rangle$. From here it is easy to

obtain,

$$|\alpha|^2 = \frac{1+A}{2}, \quad |\beta|^2 = \frac{1-A}{2}. \quad (\text{B6})$$

Two independent wave functions are then obtained as,

$$|\chi_n\rangle_1 = \sqrt{\frac{1+A}{2}} |+\rangle + \sqrt{\frac{1-A}{2}} |-\rangle, \quad (\text{B7})$$

$$|\chi_n\rangle_2 = \sqrt{\frac{1+A}{2}} |+\rangle - \sqrt{\frac{1-A}{2}} |-\rangle. \quad (\text{B8})$$

These two wave functions have the same spin mean value, $\langle \hat{S}_z \rangle_{\text{System}}$, but they are not orthogonal, unless $|\alpha| = |\beta| = 1/\sqrt{2}$. For $|\alpha| \neq |\beta|$, it is straightforward to obtain the orthogonal partner for each of these wave functions, but for their orthogonal partner the spin mean value is no longer $\langle \hat{S}_z \rangle_{\text{System}}$.

We discuss now how this result affects our evaluation of the total neutrino-neutron scattering cross section. For convenience, we start with the unpolarized case ($A = 0$). In Sec. II A, our result for $\langle |\mathcal{M}_{\nu n', \nu n}|^2 \rangle$ is given in Eq. (14), where the average over initial states is done with $|+\rangle$ and $|-\rangle$, having each state the same weight. As long as we employ a set of complete orthonormal states, the choice of the states is arbitrary. If we consider the following states (instead of $|+\rangle$ and $|-\rangle$),

$$\begin{aligned} |\chi_{n(A=0)}\rangle_1 &= \frac{1}{\sqrt{2}}(|+\rangle + |-\rangle), \\ |\chi_{n(A=0)}\rangle_2 &= \frac{1}{\sqrt{2}}(|+\rangle - |-\rangle), \end{aligned} \quad (\text{B9})$$

which are obtained from Eqs. (B7) and (B8) by making $A = 0$, then we obtain the same result as in Eq. (14).

This last point is somehow subtle and deserves a detailed explanation to avoid confusion. We can evaluate $\langle |\mathcal{M}_{\nu n', \nu n}|^2 \rangle$ by using a single spin wave function (then no average is needed), as long as this spin wave function has already the correct spin mean value. To do so, we employ Eq. (10) and

we choose $|\chi_{n(A=0)}\rangle_1$ as the initial neutron spin state. The hadron tensor represents the square of a transition amplitude. First, $H_{\mu\alpha}^+$ ($H_{\mu\alpha}^-$) projects $|\chi_{n(A=0)}\rangle_1$ into its spin up (down) component, which is $|+\rangle/\sqrt{2}$ ($|-\rangle/\sqrt{2}$) and then each contribution is squared, given a common factor $1/2$ for both the spin up and down configurations. As expected, the final results is the one in Eq. (14), but the procedure have been different. In Sec. II A, we averaged the result for $\langle |\mathcal{M}_{\nu n', \nu n}|^2 \rangle$ from two different states, $|+\rangle$ and $|-\rangle$. In the present case, we employ one single state whose spin mean value is zero. We can repeat the procedure with $|\chi_{n(A=0)}\rangle_2$, having the same result, as the relative phase plays no role for this problem. The average of two identical quantities is the same quantity. Note also that we are using nonrelativistic spin wave functions. This is because our starting point (the spin mean value from the EoS) is nonrelativistic. Having in mind that our results are nonrelativistic, we consider that this is a reasonable approximation.

Finally, we consider the polarized case ($A \neq 0$). From the discussion in the last paragraph, the result for the polarized case is almost straightforward. We have two independent states $|\chi_n\rangle_1$ and $|\chi_n\rangle_2$, which fulfill the correct average requirement and, up to the physical process considered in this work, we have the freedom to choose between one or the other. Therefore, we can take either $|\chi_n\rangle_1$ or $|\chi_n\rangle_2$, and we discard the orthogonal partner in the evaluation of $\langle |\mathcal{M}_{\nu n', \nu n}|^2 \rangle$ due to it spin mean value, which, as it was said, is different from $\langle \hat{S}_z \rangle_{\text{System}}$.

From these considerations, we conclude that $\langle |\mathcal{M}_{\nu n', \nu n}^+|^2 \rangle$ should be weighted with a factor $|\alpha|^2$ and $\langle |\mathcal{M}_{\nu n', \nu n}^-|^2 \rangle$ with a factor $|\beta|^2$. The total cross section would read then,

$$\frac{\sigma(p_\nu)}{V} = \left(\frac{1+A}{2} \right) \frac{\sigma^+(p_\nu)}{V} + \left(\frac{1-A}{2} \right) \frac{\sigma^-(p_\nu)}{V}. \quad (\text{B10})$$

From here it is easy to find the total neutrino mean free path, which is given in Eq. (28).

-
- [1] H. A. Bethe, *Rev. Mod. Phys.* **62**, 801 (1990).
[2] Th. Janka and E. Müller, *Astron. Astrophys.* **306**, 167 (1996).
[3] A. Burrows, *Nature (London)* **403**, 727 (2000).
[4] A. Burrows and J. M. Lattimer, *Astrophys. J. Suppl.* **307**, 178 (1986).
[5] H.-Th. Janka and E. Müller, *Astrophys. J. Suppl.* **448**, L109 (1995).
[6] Y. A. Shibbanov and D. G. Yakovlev, *Astron. Astrophys.* **309**, 171 (1996).
[7] D. G. Yakovlev and C. J. Pethick, *Annu. Rev. Astron. Astrophys.* **42**, 169 (2004).
[8] A. Perego, S. Rosswog, R. Cabezón, O. Korobkin, R. Kaepfeli, A. Arcones, and M. Liebendoerfer, *Mon. Not. R. Astron. Soc.* **443**, 3134 (2014).
[9] D. Martin, A. Perego, A. Arcones, F.-K. Thielemann, O. Korobkin, and S. Rosswog, *Astrophys. J.* **813**, 2 (2015).
[10] M. Frensel, M.-R. Wu, C. Volpe, and A. Perego, *Phys. Rev. D* **95**, 023011 (2017).
[11] I. Bombaci, *Astron. Astrophys.* **305**, 871 (1996).
[12] M. Prakash, I. Bombaci, M. Prakash, P. J. Ellis, J. M. Lattimer, and R. Knorren, *Phys. Rep.* **280**, 1 (1997).
[13] D. G. Yakovlev, A. D. Kaminker, O. Y. Gnedin, and P. Haensel, *Phys. Rep.* **354**, 1 (2001).
[14] R. C. Duncan and C. Thompson, *Astrophys. J.* **392**, L9 (1992).
[15] I. Sagert and J. Schaffner-Bielich, *Astron. Astrophys.* **489**, 281 (2008).
[16] A. Kusenko and G. Segrè, *Phys. Rev. Lett.* **77**, 4872 (1996).
[17] C. J. Horowitz and G. Li, *Phys. Rev. Lett.* **80**, 3694 (1998).
[18] V. L. Kauts, A. M. Savochkin, and A. I. Studenikin, *Phys. At. Nucl.* **69**, 1453 (2006).
[19] D. Tubbs and D. Schramm, *Astrophys. J.* **201**, 467 (1975).
[20] R. F. Sawyer, *Phys. Rev. D* **11**, 2740 (1975).
[21] N. Iwamoto and C. J. Pethick, *Phys. Rev. D* **25**, 313 (1982).
[22] S. O. Bäckman, C. G. Källman, and O. Sjöberg, *Phys. Lett.* **43B**, 263 (1973).
[23] P. Haensel and A. J. Jerzak, *Astron. Astrophys.* **179**, 127 (1987).
[24] S. Reddy, M. Prakash, J. M. Lattimer, and J. A. Pons, *Phys. Rev. C* **59**, 2888 (1999).

- [25] C. J. Horowitz and K. Wehrberger, *Nucl. Phys. A* **531**, 665 (1991).
- [26] S. Reddy and M. Prakash, *Astrophys. J.* **478**, 689 (1997).
- [27] S. Reddy, M. Prakash, and J. M. Lattimer, *Phys. Rev. D* **58**, 013009 (1998).
- [28] S. Reddy, Ph.D. thesis, State University of New York at Stony Brook, 1998.
- [29] A. Burrows and R. F. Sawyer, *Phys. Rev. C* **58**, 554 (1998).
- [30] J. Navarro, E. S. Hernández, and D. Vautherin, *Phys. Rev. C* **60**, 045801 (1999).
- [31] C. Shen, U. Lombardo, N. Van Giai, and W. Zuo, *Phys. Rev. C* **68**, 055802 (2003).
- [32] J. Margueron, I. Vidaña, and I. Bombaci, *Phys. Rev. C* **68**, 055806 (2003).
- [33] V. G. Bezchastnov and P. Haensel, *Phys. Rev. D* **54**, 3706 (1996).
- [34] D. A. Baiko and D. G. Yakovlev, *Astron. Astrophys.* **342**, 192 (1999).
- [35] P. Arras and D. Lai, *Phys. Rev. D* **60**, 043001 (1999).
- [36] D. Chandra, A. Goyal, and K. Goswami, *Phys. Rev. D* **65**, 053003 (2002).
- [37] S. Ando, *Phys. Rev. D* **68**, 063002 (2003).
- [38] C. J. Horowitz and A. Schwenk, *Phys. Lett. B* **642**, 326 (2006).
- [39] M. A. Pérez-García, *Phys. Rev. C* **80**, 045804 (2009).
- [40] M. A. Pérez-García, *Eur. Phys. J. A* **44**, 77 (2010).
- [41] R. B. Wiringa, V. G. J. Stoks, and R. Schiavilla, *Phys. Rev. C* **51**, 38 (1995).
- [42] B. S. Pudliner, V. R. Pandharipande, J. Carlson, and R. B. Wiringa, *Phys. Rev. Lett.* **74**, 4396 (1995).
- [43] L. G. Cao, U. Lombardo, C. W. Shen, and N. V. Giai, *Phys. Rev. C* **73**, 014313 (2006).
- [44] C. J. Joachin, *Quantum Collision Theory* (North-Holland, Amsterdam, 1975).
- [45] R. Aguirre, E. Bauer, and I. Vidaña, *Phys. Rev. C* **89**, 035809 (2014).
- [46] I. Vidaña and I. Bombaci, *Phys. Rev. C* **66**, 045801 (2002).
- [47] T. Maruyama, M. K. Cheoun, J. Hidaka, T. Kajino, T. Kuroda, G. J. Mathews, C. Y. Ryu, T. Takiwaki, and N. Yasutake, *Phys. Rev. D* **90**, 067302 (2014).
- [48] E. Rrapaj, J. W. Holt, A. Bartl, S. Reddy, and A. Schwenk, *Phys. Rev. C* **91**, 035806 (2015).
- [49] D. Griffiths, *Introduction to Elementary Particles*, 2nd ed. (Wiley-VCH, New York, 2008).
- [50] C. Cohen-Tannoudji, B. Diu, and F. Laloë, *Quantum Mechanics* (Hermann and John Wiley & Sons, New York, 1977).